

*Methods*

# Beyond the patch-clamp resolution: functional activity of nonelectrogenic vacuolar NHX proton/potassium antiporters and inhibition by phosphoinositides

Antonella Gradogna<sup>1</sup> , Joachim Scholz-Starke<sup>1</sup> , José M. Pardo<sup>2</sup>  and Armando Carpaneto<sup>1,3</sup> <sup>1</sup>Institute of Biophysics, National Research Council, Via De Marini 6, Genova 16149, Italy; <sup>2</sup>Institute of Plant Biochemistry and Photosynthesis, CSIC-University of Seville, Seville 41092, Spain; <sup>3</sup>Department of Earth, Environment and Life Sciences (DISTAV), University of Genoa, Viale Benedetto XV 5, Genova 16132, Italy

Author for correspondence:

Armando Carpaneto

Email: armando.carpaneto@unige.it

Received: 29 July 2020

Accepted: 12 October 2020

New Phytologist (2021) 229: 3026–3036  
doi: 10.1111/nph.17021**Key words:** BCECF, fluorescence, NHX antiporters, patch-clamp, PI(3,5)P<sub>2</sub>, plant vacuole, proton.

## Summary

- We combined the patch-clamp technique with ratiometric fluorescence imaging using the proton-responsive dye BCECF as a luminal probe.
- Upon application of a steep cytosol-directed potassium ion (K<sup>+</sup>) gradient in Arabidopsis mesophyll vacuoles, a strong and reversible acidification of the vacuolar lumen was detected, whereas no associated electrical currents were observed, in agreement with electroneutral cation/H<sup>+</sup> exchange.
- Our data show that this acidification was generated by NHX antiport activity, because: it did not distinguish between K<sup>+</sup> and sodium (Na<sup>+</sup>) ions; it was sensitive to the NHX inhibitor benzamil; and it was completely absent in vacuoles from *nhx1 nhx2* double knockout plants. Our data further show that NHX activity could be reversed, was voltage-independent and specifically impaired by the low-abundance signaling lipid PI(3,5)P<sub>2</sub>, which may regulate salt accumulation in plants by acting as a common messenger to coordinately shut down secondary active carriers responsible for cation and anion uptake inside the vacuole.
- Finally, we developed a theory based on thermodynamics, which supports the data obtained by our novel experimental approach.
- This work, therefore, represents a proof-of-principle that can be applied to the study of proton-dependent exchangers from plants and animals, which are barely detectable using conventional techniques.

## Introduction

The patch-clamp technique consists of attaching a glass pipette with a micrometric tip to the cell membrane (Neher & Sakmann, 1976). The application of a light suction induces an extremely tight contact (seal) between the pipette and the membrane with a resistance that can reach values of about ten billion ohms and more. This leads to a drastic reduction of the background noise, inversely proportional to the resistance (Hamill *et al.*, 1981), and to the possibility of recording, through appropriate precautions, signals of the order of femtoamperes (Carpaneto *et al.*, 2005). In the case of plant cells, it is first necessary to remove the cell wall, usually by enzymatic treatment. Because it is difficult to control how 'clean' the plasma membrane is, the patch clamp is difficult to apply on protoplasts. However, vacuoles are an ideal preparation, because they are easy to isolate, large in size, and the incidence of obtaining a giga seal between pipette and tonoplast is very high (Gradogna *et al.*, 2009; Costa *et al.*, 2012; Festa *et al.*, 2016; Lagostena *et al.*, 2017). Recently, using the pH-sensitive

fluorescent dye 2',7'-Bis(2-carboxyethyl)-5(6)-carboxyfluorescein (BCECF), it has been possible to determine that the activity of the vacuolar nitrate/proton antiporter CLC-a is reflected in the vacuolar pH value (Carpaneto *et al.*, 2017). We hypothesized that a similar approach could be used for the functional characterization of nonelectrogenic secondary transporters, such as NHX transporters.

NHX (sodium ion /proton (Na<sup>+</sup>/H<sup>+</sup>) eXchangers) is a family of cation/proton antiporters belonging to clade CPA1, one of the two groups that form the CPA superfamily (Cation/Proton Antiporters, Chanroj *et al.*, 2012). They are believed to be involved in various physiological processes such as pH and potassium homeostasis, plant growth and salt stress acclimation (Reguera *et al.*, 2014). In Arabidopsis, there are eight isoforms divided into three groups: AtNHX1–4 are located at the vacuole, AtNHX5/6 in intracellular compartments and AtNHX7/8 at the plasma membrane. With regard to AtNHX1–4, expressed at the vacuole, experiments on single isoform or multiple knockout plants (Bassil *et al.*, 2011, 2019; Barragán *et al.*, 2012) have

shown that NHX1 and 2 are responsible for the observed phenotypes (plants lacking both NHX1 and 2 were severely impaired in growth and extremely sensitive to external potassium changes), whereas the role of NHX3 and 4 is secondary, with a likely low functional activity. Here, we used vacuoles isolated from mesophyll cells of *Arabidopsis thaliana* wild-type plants, *clc-a* and *nhx1 nhx2* mutants and, applying the patch-clamp technique combined with the fluorescence signal of the proton indicator dye BCECF, we measured the functional activity of AtNHX1 and 2 and studied their pharmacological properties. Indeed, we show that the signaling lipid phosphatidylinositol-3,5-bisphosphate (PI(3,5)P<sub>2</sub>) strongly inhibits NHX activity. This novel approach, therefore, is capable of investigating electroneutral vacuolar cation/H<sup>+</sup> exchange processes in unprecedented detail.

## Materials and Methods

Supporting Information Fig. S1 shows a schematic presentation of the materials and methods used in this work.

### Plant material

Plants of *Arabidopsis thaliana clc-a* knockout, Columbia-0 wild-type (WT), *nhx1 nhx2* knockout, *tpc1-2* mutants (two-pore channel 1, AtTPC1, null background; Peiter *et al.*, 2005) were grown on soil in a growth chamber at 22°C and 8 h : 16 h, light : dark regime. For isolation of mesophyll protoplasts, leaves from 3–5-week-old plants were cut in strips, placed in a Petri dish and enzymatically digested for 1 h at 22°C in the dark. The enzyme solution contained: 0.5% Cellulase Onozuka R-10 (Yakult), 0.05% Pectolyase Y-23 (Seishin), 0.25% Macerozyme R-10, 1 mM CaCl<sub>2</sub>, 500 mM D-sorbitol, 10 mM MES, pH 5.5. The protoplast suspension was filtered through 50-µm nylon mesh, subsequently centrifuged and washed twice in the so-called W5 (see Yoo *et al.*, 2007) solution containing (in mM): 125 CaCl<sub>2</sub>, 154 NaCl, 5 KCl, 2 MES-KOH, 5 glucose, pH 5.6 and 640 mOsm. The protoplast pellet was suspended in W5 solution and maintained at 4°C for 1–3 d. Just before patch-clamp experiments, 20–30 µl of W5 solution containing the protoplasts were placed in the recording chamber and exposed to the vacuolar release solution (VRS) containing (in mM): 100 malic acid, 155 Bis-tris-Propane (BTP), 5 ethylene glycol-bis(2-aminoethylether)-N,N,N',N'-tetraacetic acid (EGTA), 3 MgCl<sub>2</sub>, 200 D-sorbitol, pH 7.33. Vacuoles were efficiently released from the protoplasts within 3–5 min.

### Patch-clamp recordings

Because CLC-a is known to affect vacuolar pH, to measure *bona fide* NHX activity, *clc-a* knockout plants were selected to perform experiments, unless otherwise indicated.

Patch-clamp recordings were performed in the whole-vacuole configuration. The standard pipette solution contained (in mM): 100 KCl, 3 MgCl<sub>2</sub>, 10 µM 2',7'-bis-(2-carboxyethyl)-5-(and-6)-carboxyfluorescein (BCECF), 240 D-sorbitol, pH 7.0 (with KOH). The standard cytosolic bath solution contained (in mM):

100 KCl, 3 MgCl<sub>2</sub>, 5 Hepes, 280 D-sorbitol, pH 7.2 (with KOH). To establish a steep potassium gradient between the vacuolar lumen and the cytosol, potassium in the standard bath solution was replaced by equimolar concentration of sodium (no K<sup>+</sup> + Na<sup>+</sup>), caesium (no K<sup>+</sup> + Cs<sup>+</sup>) or Bis-Tris Propane abbreviated to BTP (no K<sup>+</sup> + BTP<sup>+</sup>), and the relative hydroxide was used for pH buffering. In the case of BTP, which is itself a proton buffer, the solution was: (in mM): 100 HCl, 69 BTP, 3 MgCl<sub>2</sub>, 300 D-sorbitol, pH 7.2.

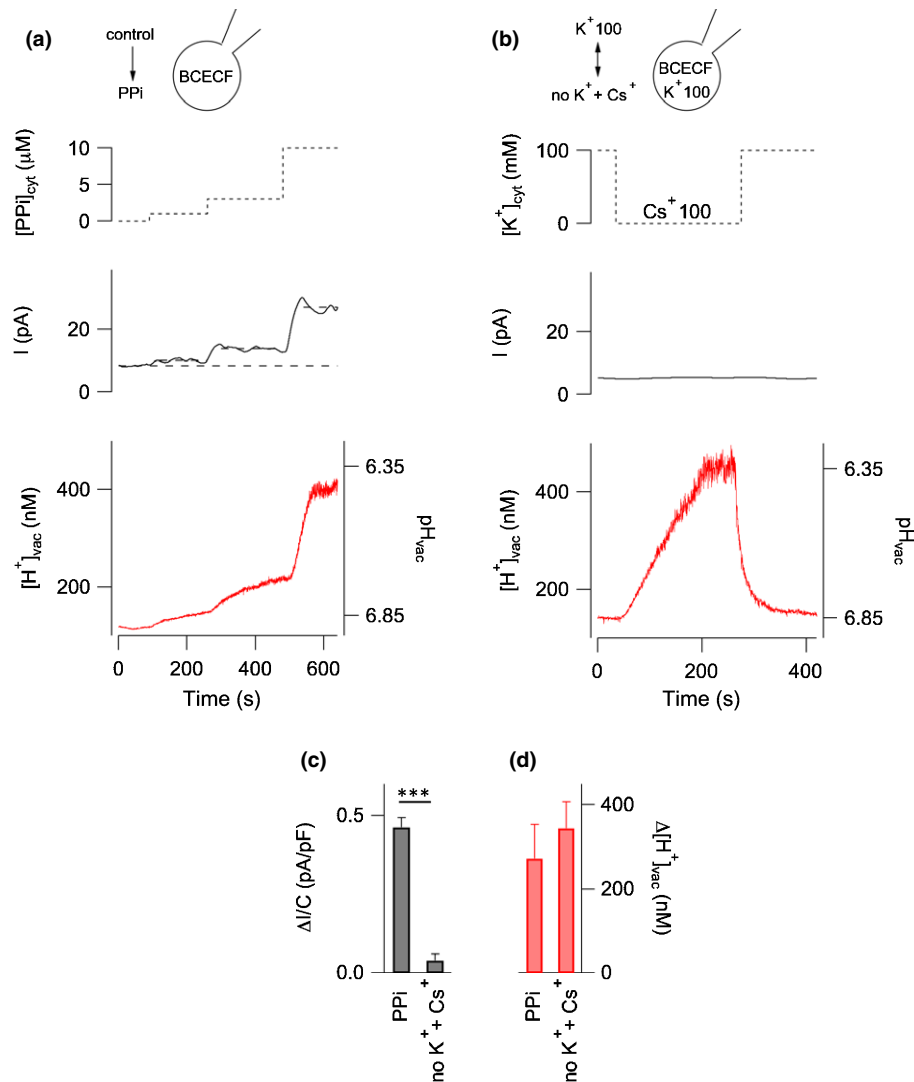
In order to test the reliability of the system to detect patch-clamp currents and pH changes at the same time, vacuolar proton-pumping pyrophosphatase was activated by inorganic pyrophosphate (PPi). Potassium pyrophosphate was prepared as a 100 mM aqueous stock solution, stored at –20°C and dissolved in the standard bath solution at the desired concentration.

Benzamil hydrochloride was prepared as a 50 mM DMSO stock solution. It was stored at –20°C and freshly dissolved at 30 µM concentration in no K<sup>+</sup> + BTP<sup>+</sup> solution. Water-soluble dioctanoyl esters (diC8) of PI(4,5)P<sub>2</sub>, PI(3,4)P<sub>2</sub>, PI(3,4,5)P<sub>3</sub>, PI(3,5)P<sub>2</sub> (Echelon Biosciences Inc., Salt lake City, UT, USA) were prepared as 1 mM aqueous stock solutions. They were stored at –20°C and dissolved at 200 nM concentration in no K<sup>+</sup> + BTP<sup>+</sup> solution just before use.

In the experiments of Fig. 5 (see later), the pipette solution contained (in mM): 100 CsCl, 3 MgCl<sub>2</sub>, 10 µM BCECF, 240 D-sorbitol, pH 7.0 (with CsOH). The cytosolic bath solution contained (in mM): 100 CsCl, 3 MgCl<sub>2</sub>, 5 Hepes, 280 D-sorbitol, pH 7.2 (with CsOH) and was substituted by the standard bath solution in order to establish a steep potassium gradient between the cytosol and the vacuolar lumen. Patch pipettes were pulled from borosilicate glass capillaries (Harvard Apparatus, Holliston, MA, USA) and had resistances of 3–5 MΩ. For patch-clamp experiments, vacuoles were placed in the recording chamber and observed by an inverted microscope (Zeiss) with a ×40 objective (overall magnification ×400). Currents were recorded with a List EPC-7 amplifier (Darmstadt, Germany) at holding potential of 0 mV or, when specified, –40 mV, filtered with a low pass Bessel filter (Sakmann & Neher, 1995) and controlled by the acquisition program Pulse (Heka Elektronik, Lambrecht, Germany). The perfusion system was optimized to change the bath solution in approx. 1 min and consisted of a gravity perfusion system for inflow and a peristaltic pump for outflow (Gilson Inc., Middleton, WI, USA). The effects of perfusion on the kinetics of the luminal proton concentration are treated in detail in Notes S1 Theory. In the main figures (Figs 1–6), traces of pyrophosphate or cytosolic K concentrations (drawn as dotted lines) just indicate the switching of the corresponding bath solution. Membrane capacitance (C<sub>v</sub>) and access resistance (R<sub>a</sub>) could be estimated by the current transient elicited by a 10 mV voltage pulse (Sakmann & Neher, 1995). By convention, positive currents correspond to cations moving from the cytosolic side to the vacuolar lumen.

### BCECF fluorescence

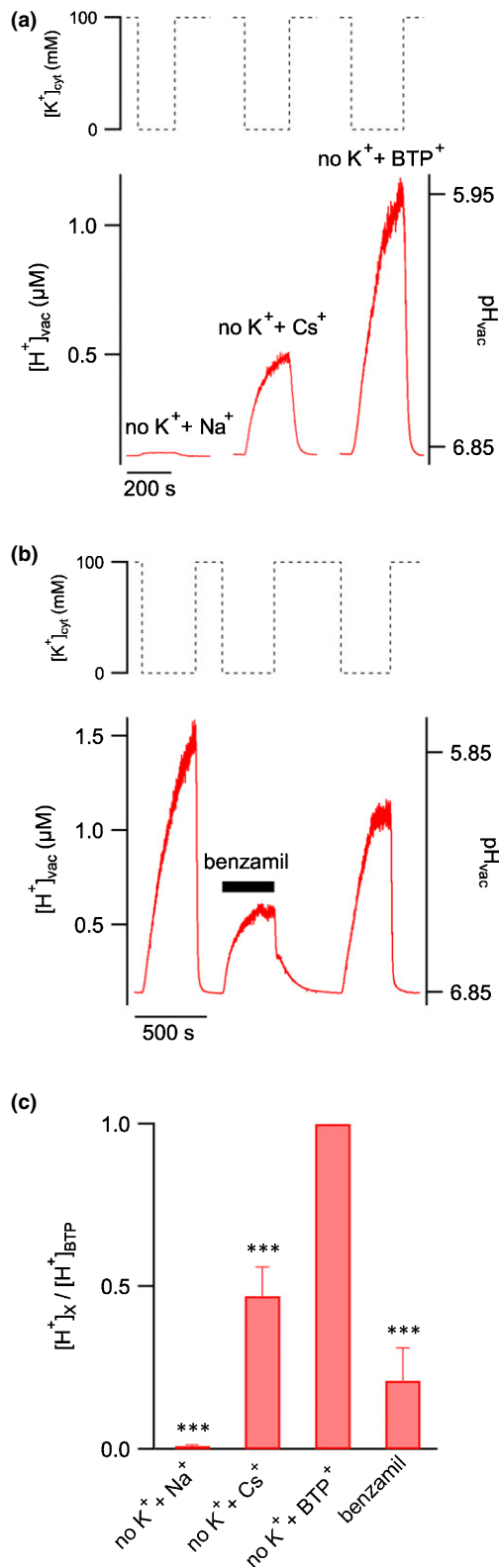
After reaching the whole-vacuole configuration, vacuole loading by BCECF took from 10 to 30 min, as shown in Fig. S2



**Fig. 1** Vacuolar acidification induced by a cytosol-directed potassium gradient. (a) Upon addition of inorganic pyrophosphate (PPI) at concentrations of 1, 3 and 10  $\mu\text{M}$  to the bath solution (top panel), the time course of vacuolar membrane current (middle panel) was recorded by patch-clamp and luminal proton concentration (bottom panel) was evaluated by 2',7'-Bis(2-carboxyethyl)-5(6)-carboxyfluorescein (BCECF) fluorescence ratio signal (see the Materials and Methods section for details). Jumps in the dotted lines indicate the switching of the bath solution irrespective to the real change due to the perfusion system (see Supporting Information Notes S1 Theory and the Materials and Methods section for a discussion about the effects of the perfusion). (b) When in the cytosolic bath solution potassium was removed (top panel, no  $\text{K}^+ + \text{Cs}^+$ , 100 mM  $\text{K}^+$  was substituted by an equimolar amount of caesium ions ( $\text{Cs}^+$ )) and a patch-clamp was applied on a vacuole isolated from *Arabidopsis mesophyll* cells, no change in background current was apparent (middle panel); the concentration of luminal potassium was 100 mM. However, the proton-sensitive fluorescent dye BCECF loaded inside the vacuole through the patch pipette indicated a significant acidification (bottom panel). (c) Average current changes, normalized to the vacuolar capacitance ( $\Delta I/C$ ), induced by removal of cytosolic potassium (no  $\text{K}^+ + \text{Cs}^+$ ,  $n = 4$ ) or by the addition of 10  $\mu\text{M}$  pyrophosphate (PPI,  $n = 3$ ). Significance: \*\*\*,  $P < 0.001$ . (d) Comparison of the average increase in proton concentration by removal of cytosolic potassium (no  $\text{K}^+ + \text{Cs}^+$ ,  $n = 4$ ) and by addition on the cytosolic bath solution of 10  $\mu\text{M}$  pyrophosphate (PPI,  $n = 3$ ). Measurements were performed on vacuoles isolated from *Arabidopsis clc-1* knockout plants.

(diffusion from the patch pipette to the whole cell-wall-free protoplasts also was investigated by Goh *et al.*, 2002, and cited papers). Simultaneous whole-vacuole patch-clamp recordings and fluorescence detection then were performed. Excitation light, alternately selected by a monochromator (Cairn Research, Faversham, UK) at 490 and 440 nm in 100 ms excitation cycles, was generated by a Xenon arc lamp (PTI). Fluorescence emission was detected using a 515-nm bandpass emission filter and recorded every 300 ms by a CCD camera

(Roper Scientific GmbH, Ottobrun, Germany) mounted on an inverted microscope (Axiovert, Zeiss). The fluorescence ratio (490/440) was calculated online in a selected circular region of interest (ROI) placed inside the vacuole, as shown in Fig. S4(a). Background fluorescence usually was negligible or, otherwise, was subtracted off-line. In our experimental conditions, BCECF signals were very stable over a long period,  $\leq 4500$  s after the loading phase, see as an example Fig. S4(b), thus indicating negligible photobleaching.



**Fig. 2** Modulation of the potassium gradient ( $\Delta K^+$ )-mediated vacuolar acidification. (a) Potassium in the standard cytosolic bath solution was replaced with an equal concentration of sodium (no  $K^+$  +  $Na^+$ ), caesium (no  $K^+$  +  $Cs^+$ ) or Bis-tris-Propane (BTP) (no  $K^+$  +  $BTP^+$ ). The corresponding vacuolar acidification is shown in the lower panel. (b) When 30  $\mu\text{M}$  benzamil was added to the solution without potassium (no  $K^+$  +  $BTP^+$  solution), a significant reduction of the vacuolar acidification was recorded. The effect was partially reversible as shown by the increase in  $[H^+]_{\text{vac}}$  after perfusion with the  $\Delta K^+$  solution without the inhibitor. (c) Variation in vacuolar proton concentration ( $\Delta[H^+]_{\text{vac}}$ ) normalized to the change in vacuolar proton concentration ( $\Delta[H^+]_{\text{BTP}}$ ) mediated by application of no  $K^+$  +  $BTP^+$  solution. Potassium in standard cytosolic bath solution was replaced respectively by sodium (no  $K^+$  +  $Na^+$ ,  $n = 8$ ) and caesium (no  $K^+$  +  $Cs^+$ ,  $n = 4$ ) or 30  $\mu\text{M}$  Benzamil was added in no  $K^+$  +  $BTP^+$  solution ( $n = 5$ ). Significance: \*\*\*,  $P < 0.001$ . The average value of  $\Delta[H^+]_{\text{BTP}}$  was  $7.3 \pm 0.7 \times 10^{-7} \text{ M}$  ( $n = 23$ ). Measurements were performed on vacuoles isolated from Arabidopsis *clc-a* knockout plants.

droplet of the buffered solution was recorded. The surface of the droplet was flat to avoid undesired light scattering and reflection. A plot of proton concentration vs fluorescence ratio was generated and data were fitted with an exponential function, Fig. S5. Parameters of the fit were used to convert experimental fluorescence ratios into proton concentration units. Previous data (see fig. EV3 in Carpaneto *et al.*, 2017) ensured that the same type of calibration performed in whole-vacuole configuration would have produced similar conversion values.

### Statistical analysis

All results were gained from three or more independent experiments. Results are given as mean  $\pm$  standard error (SE). For statistical analysis and graph preparations the software IGOR PRO (WaveMetrics Inc., Lake Oswego, OR, USA) and EXCEL (Microsoft Corp., Redmond, WA, USA) were used. Student's *t*-test was used for statistical comparison between means where applicable: \*,  $P < 0.05$ ; \*\*,  $P < 0.01$ ; \*\*\*,  $P < 0.001$ .

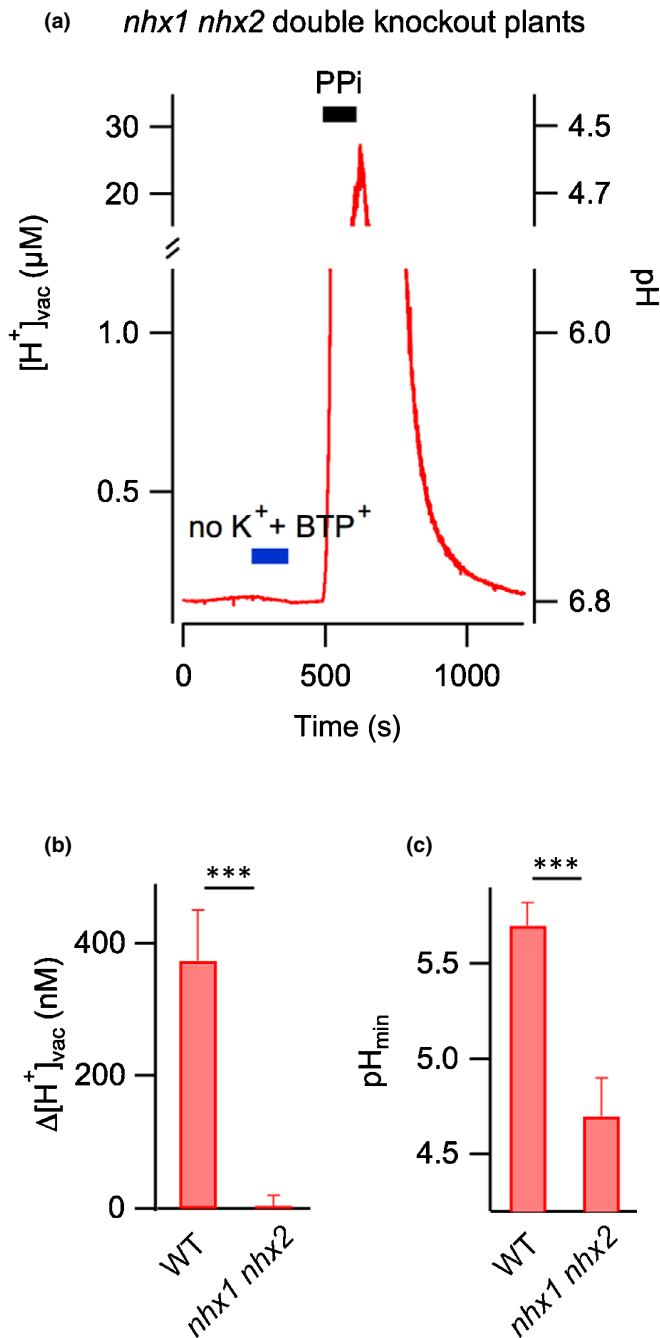
### Results

In order to detect  $H^+$ -dependent ion transport across the membrane of vacuoles isolated from *A. thaliana* mesophyll cells, we combined the patch-clamp technique with fluorescence ratio recordings using the ratiometric  $H^+$  indicator dye BCECF (for a schematic overview on experiment preparation and execution, see Fig. S1). The ionic solution in the patch pipette contained the fluorophore (concentration 10  $\mu\text{M}$ ) able to detect proton concentration changes. After gaining access to the whole-vacuole configuration, the fluorescent dye diffused into the vacuolar lumen; this loading phase lasted from 10 to 30 min (Fig. S2) and was dependent on both the size of the vacuole, monitored by the electrical membrane capacitance ( $C_m$ ) and on  $R_a$ . Recordings were started after this lag period when the pH inside of the vacuole was stable.

In order to test the reliability of our experimental system, we performed a series of experiments in which PPI was added to the cytosolic bath solution (Fig. 1a, upper panel). Because it is known that CLC-a is an active player in modulating vacuolar pH (De

For calibration of the fluorescence ratios, a 50 mM buffer at a fixed pH was added to the vacuolar solution containing 10  $\mu\text{M}$  BCECF (sequentially: HEPES at pH 7, MES at pH 6.5, MES at pH 5.5 and Citrate at pH 3.5) and the fluorescence of a 500  $\mu\text{l}$





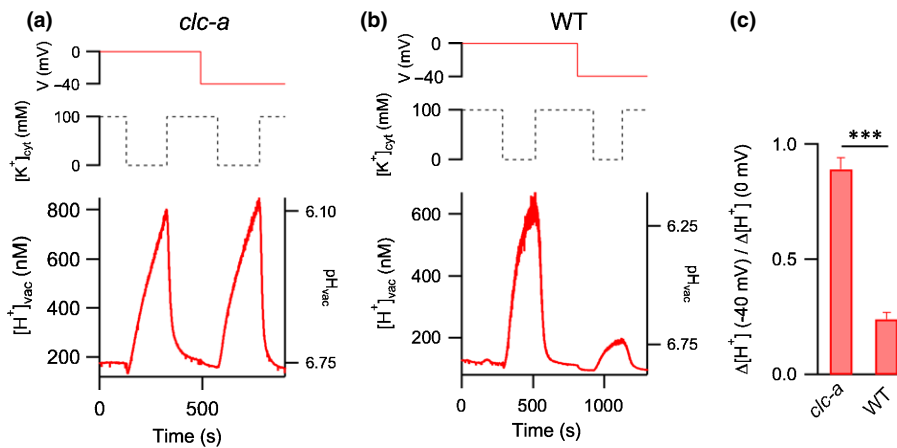
**Fig. 3** The potassium gradient ( $\Delta K^+$ )-induced vacuolar acidification was mediated by AtNHX1 and AtNHX2. (a) No significant change in proton luminal concentration was observed when potassium was replaced by Bis-tris-Propane (BTP) (no  $K^+$  + BTP $^+$ , blue line) in the solution bathing a patched vacuole isolated from mesophyll cells of Arabidopsis double mutant *nhx1 nhx2* plants; when 100  $\mu M$  PPI was added to the standard control solution, a strong acidification was apparent. (b) Change in proton concentration mediated by the application of no  $K^+$  + BTP $^+$  solution in vacuoles from Columbia (wild-type, WT) and double mutant *nhx1 nhx2* (*nhx1 nhx2*) plants (WT,  $n=5$ ; *nhx1 nhx2*,  $n=9$ ). \*\*\*,  $P < 0.001$ . (c) Comparison of the minimum pH detected in vacuoles from Columbia (WT) and double mutant *nhx1 nhx2* (*nhx1 nhx2*) plants after addition of 100  $\mu M$  PPI to the standard control solution (WT,  $n=12$ ; *nhx1 nhx2*,  $n=9$ ). Significance: \*\*\*,  $P < 0.001$ .

Angeli *et al.*, 2006; Carpaneto *et al.*, 2017), experiments in Fig. 1 were performed on vacuoles isolated from *clc-a* knockout plants. Owing to the well-known activity of the  $H^+$ -pumping pyrophosphatase, PPI applied at 1, 3 and 10  $\mu M$  elicited positive currents of increasing amplitudes, as shown in the middle panel of Fig. 1(a), together with a contemporary increase in vacuolar proton concentration (Fig. 1a, lower panel). We then applied a different experimental protocol in which the standard bath solution (cytosolic side) was changed by completely removing  $K^+$  ions, substituted by an equimolar concentration of caesium, (no  $K^+$  +  $Cs^+$ ), as shown in the upper panel of Fig. 1(b), therefore generating a large potassium gradient ( $\Delta K^+$ ) from the lumen ( $[K^+]_{lumen} = 100$  mM) to the cytosolic side of the vacuole ( $[K^+]_{cytosol} = 0$  mM). The diffusion coefficient of caesium,  $D(Cs^+) = 2.03 \cdot 10^{-5} \text{ cm}^2 \text{ s}^{-1}$ , is very similar to that of potassium,  $D(K^+) = 1.96 \cdot 10^{-5} \text{ cm}^2 \text{ s}^{-1}$  (Hille, 2001); this limits unwanted artifactual effects on the recorded currents due to liquid junction potentials. The respective current signal, recorded by voltage-clamping the tonoplast at 0 mV, did not show any significant variation (Fig. 1b, middle panel). However, the proton concentration inside the vacuole rose from about 140 nM (pH 6.85) to 450 nM (pH 6.35) (Fig. 1b, lower panel). The effect was fully reversible and the initial pH was restored after re-application of standard bath solution with 100 mM potassium. The comparison of the average values for the experiments of Fig. 1(a,b) is presented in Fig. 1(c,d): current density changes were significantly different in the two conditions (Fig. 1c), whereas the corresponding proton concentration changes were similar (Fig. 1d).

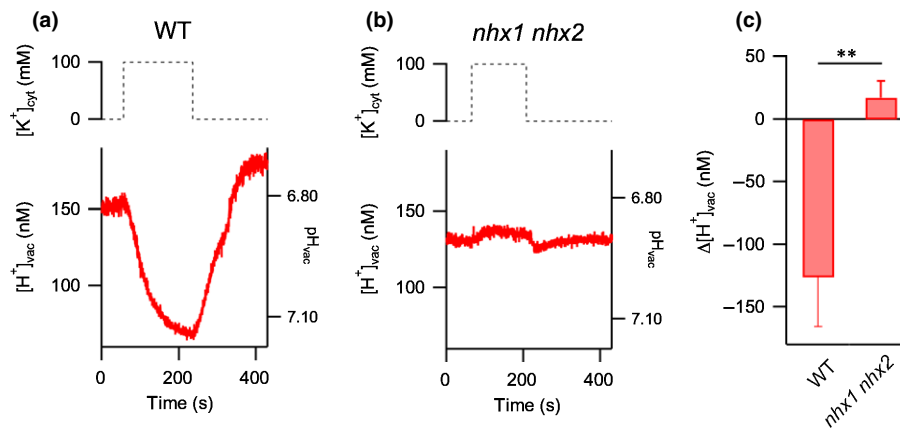
The simplest explanation for this acidification is to hypothesize the presence of a  $K^+/H^+$  exchange system driving protons from the cytosol to the lumen of the vacuole at the expense of the potassium gradient generated under 0  $K^+$  conditions; thus, a reversible  $K^+/H^+$  antiporter acting in the opposite direction than would be expected in physiological conditions in which the vacuole is acidic relative to the cytosol. Moreover, this antiporter is nonelectrogenic, with a transport stoichiometry of 1  $K^+$  : 1  $H^+$  (or multiples), because no current difference could be recorded after potassium substitution.

Vacuolar acidification was dependent on the substituting cation and inhibited by benzamil

In order to further characterize this cation antiporter, we repeated the experiments by varying the cation replacing potassium in the bath solution. Fig. 2(a) shows how the use of sodium (no  $K^+$  +  $Na^+$ ), caesium (no  $K^+$  +  $Cs^+$ ) or Bis-Tris Propane (no  $K^+$  + BTP $^+$ ) had different impacts on vacuolar acidification. Sodium hardly modified  $[H^+]_{vac}$ , whereas the large, membrane-impermeable cation BTP $^+$  induced the largest effect and was chosen for the following experiments. In this condition (no  $K^+$  + BTP $^+$ ), we recorded very small currents Fig. S3, that were not affected by the inhibitors (see below) and also were present in vacuoles isolated from *nhx1 nhx2* knockout plants. These currents therefore are not related to the phenomenology shown so far, and can reasonably be attributed to the movement of



**Fig. 4** Voltage-independence of the potassium gradient ( $\Delta K^+$ )-mediated vacuolar acidification. (a) The increase in proton luminal concentration observed when potassium in the bath solution was replaced with Bis-tris-Propane (BTP) did not change varying the holding potential from 0 mV to  $-40$  mV in a patched vacuole isolated from *Arabidopsis clc-a* knockout. (b) A significant reduction of vacuolar acidification was detected in the same conditions of (a) in a vacuole isolated from *Arabidopsis* wild-type (WT). (c) Change in vacuolar proton concentration ( $\Delta[H^+]_{vac}$ ) at  $-40$  mV normalized to the change in vacuolar proton concentration at 0 mV in vacuoles respectively from *Arabidopsis clc-a* knockout (*clc-a*,  $n = 5$ ) and Columbia (WT,  $n = 5$ ). Values were significantly different (\*\*\*,  $P < 0.001$ ).



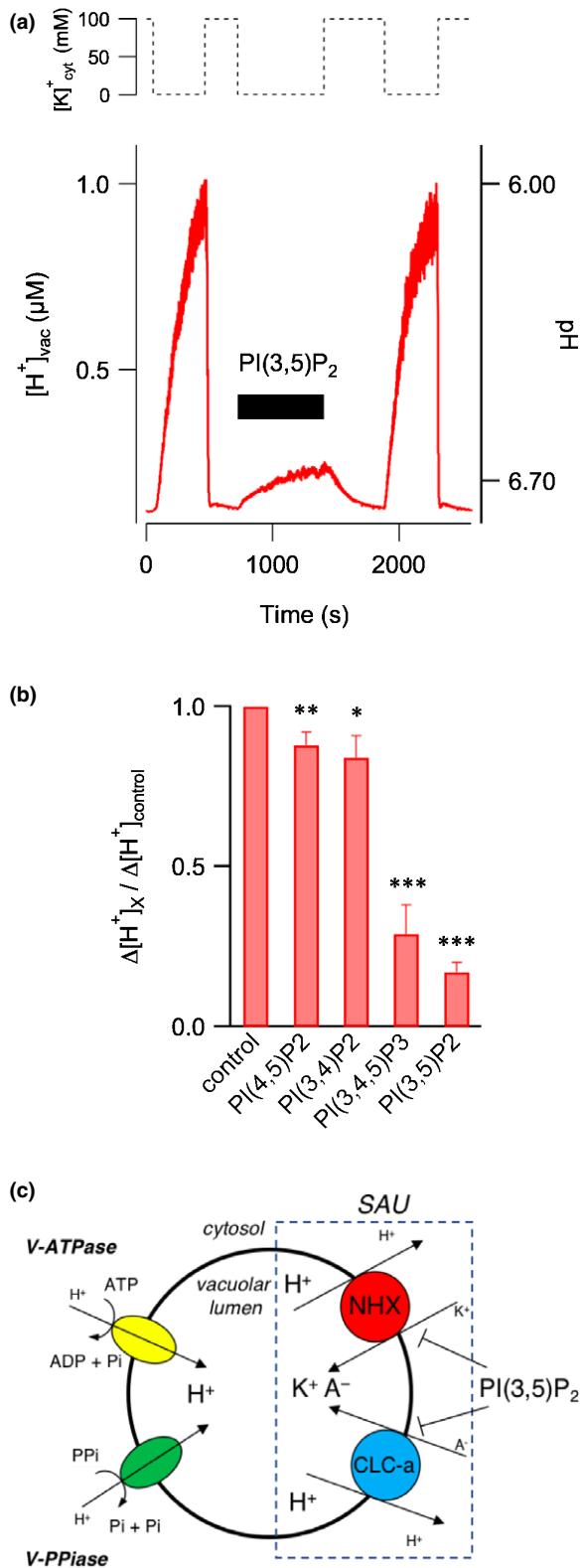
**Fig. 5** AtNHX1 and AtNHX2 can mediate vacuolar alkalinization induced by a vacuolar-directed potassium gradient in *Arabidopsis thaliana*. (a) In the absence of vacuolar potassium, a decrease in proton vacuolar concentration was detected when the bath solution containing caesium (no  $K^+ + Cs^+$ ; see the Materials and Methods section) was replaced with the standard, 100 mM potassium, bath solution. Data from vacuoles isolated from *Arabidopsis* Columbia (wild-type, WT). (b) When similar experiments were performed in vacuoles from *Arabidopsis nhx1 nhx2* double mutant no alkalinization was apparent. (c) Change in vacuolar proton concentration mediated by the replacement of caesium with potassium in the bath solution respectively in vacuoles isolated from *Arabidopsis* Columbia (WT,  $n = 8$ ) and *Arabidopsis nhx1 nhx2* double mutant (*nhx1 nhx2*,  $n = 3$ ). Values were significantly different (\*\*,  $P < 0.01$ ).

potassium through  $K^+$ -selective tonoplast channels driven by the steep potassium gradient present across the vacuolar membrane; this also is supported by the fact that no current signal was apparent when cytosolic potassium was replaced by caesium, a well-known blocker of potassium channels (see Fig. 1b, middle panel). Moreover, the experiments in no  $K^+ + Na^+$  condition (involving steep gradients of  $Na^+$  and  $K^+$  of equal magnitude, but opposite orientation; Fig. 2a) suggest that, besides being nonelectrogenic, the putative cation/ $H^+$  antiporter did not discriminate between potassium and sodium, which are biophysical features observed in NHX proteins (Venema *et al.*, 2002; Hernández *et al.*, 2009; Bassil *et al.*, 2019) Because benzamil is known as a specific inhibitor of these transporters (Venema *et al.*, 2002), we added this compound at  $30 \mu M$  concentration in the no  $K^+ + BTP^+$

solution. As shown in Fig. 2(b), a significant, partially reversible, reduction of  $K^+$ -driven vacuolar acidification was apparent. Group data of these experiments are presented in the histogram of Fig. 2(c), suggesting that NHX antiporters may be a major player in  $\Delta K^+$ -induced vacuolar acidification.

### AtNHX1 and AtNHX2 are responsible for the $\Delta K^+$ -induced vacuolar acidification

In order to verify if NHX antiporters played a relevant role in the above effects, we took advantage of *Arabidopsis* mutant lines lacking the two major forms of tonoplast-localized NHXs (i.e. NHX1 and NHX2; Bassil *et al.*, 2011; Barragán *et al.*, 2012). By using BCECF-filled pipettes, we patched vacuoles isolated from



**Fig. 6** NHX activity was inhibited by phosphoinositides. (a) The presence of 200 nM PI(3,5)P<sub>2</sub> in no K<sup>+</sup> + BTP<sup>+</sup> solution caused a strong and reversible inhibition of the vacuolar acidification mediated by NHX activity. (b) Change in proton concentration induced by the application of the no K<sup>+</sup> + BTP<sup>+</sup> solution in which different phosphoinositides were added at a concentration of 200 nM. Data were normalized to control (no K<sup>+</sup> + BTP<sup>+</sup>) condition (PI(4,5)P<sub>2</sub>,  $n = 4$ ; PI(3,4)P<sub>2</sub>,  $n = 4$ ; PI(3,4,5)P<sub>3</sub>,  $n = 6$ ; PI(3,5)P<sub>2</sub>,  $n = 7$ ). Significance: \*,  $P < 0.05$ ; \*\*,  $P < 0.01$ ; \*\*\*,  $P < 0.001$ . Measurements were performed on vacuoles isolated from Arabidopsis *clc-a* knockout plants. (c) Schematic representation of the key players in vacuolar salt uptake. NHXs together with CLC-a form a Salt Accumulation Unit (SAU). V-ATPase, vacuolar H<sup>+</sup>-ATPase; V-PPiase, vacuolar H<sup>+</sup>-pyrophosphatase. A<sup>-</sup>, H<sup>+</sup> and K<sup>+</sup> indicates respectively anions, protons and potassium ions; the dimension of the letters for the ions is proportional to their concentration.

reversible acidification. The highly significant difference between Columbia WT and *nhx1 nhx2* double mutant vacuoles in the K<sup>+</sup>-driven luminal proton increases (Fig. 3b) is a strong indication that NHX1 and NHX2 transporters are responsible for the K<sup>+</sup>/H<sup>+</sup> exchange reported by our experimental approach. Moreover, we verified that the current density of the endogenous vacuolar pyrophosphatase elicited by 100  $\mu$ M PPI is not significantly different in WT ( $1.04 \pm 0.11$  pA/pF,  $n = 12$ ) and *nhx1 nhx2* double mutant ( $0.76 \pm 0.09$  pA/pF,  $n = 9$ ) vacuoles. Therefore, the large difference in minimum luminal pH obtained by activating the pyrophosphatase (Fig. 3c) is compelling experimental evidence for the strong impact of NHX activity on the vacuolar pH, as suggested by previous studies (Bassil *et al.*, 2011; Andr s *et al.*, 2014).

#### AtNHX1 and AtNHX2 are not voltage-dependent

In order to establish if H<sup>+</sup>/K<sup>+</sup> exchange activity was dependent on the tonoplast voltage, we compared the acidification resulting from K<sup>+</sup> replacement with no K<sup>+</sup> + BTP solution at 0 and -40 mV (Fig. 4a, left panel). In vacuoles isolated from Arabidopsis *clc-a* knockout mesophyll cells, BCECF signals were similar in both conditions (Fig. 4b), indicating that AtNHXs were not voltage-dependent. However, in vacuoles isolated from Arabidopsis WT, applying the same experimental protocol, we detected a strong reduction of acidification at -40 mV compared to that at 0 mV (Fig. 4a, right panel, 4b), an effect due to the voltage-dependent activity of CLC-a, which acted to counterbalance the NHXs mediated luminal acidification (see Notes S1 Theory). These results would have been impossible to obtain by using conventional techniques (see Discussion).

#### AtNHX1 and AtNHX2 can mediate vacuolar alkalization

Our experimental data suggested that  $\Delta K^+$ -induced vacuolar acidification could be associated to NHX exchanger activity; however, in physiological conditions, NHX exchangers at the tonoplast operate to import K<sup>+</sup> into vacuoles and would be expected to drive protons from the acidic vacuole to the cytosol and not vice versa. Consequently, we wondered if we also could

Arabidopsis double mutant *nhx1 nhx2* mesophyll cells. As shown in Fig. 3(a), the removal of cytosolic potassium (no K<sup>+</sup> + BTP<sup>+</sup>) did not induce any [H<sup>+</sup>] increase in the vacuolar lumen. Instead, cytosolic application of PPI (100  $\mu$ M) caused a very large,

monitor this physiologically meaningful transport mode using our experimental approach. Therefore, in the standard pipette solution, which contained the fluorophore BCECF, potassium was replaced by caesium, as described in Materials and Methods. During the experiment, the bath solution (cytosolic side) containing 100 mM caesium was changed with the standard potassium solution thereby generating a steep potassium gradient from the cytosol ( $[K^+]_{\text{cytosol}} = 100 \text{ mM}$ ) towards the lumen ( $[K^+]_{\text{lumen}} = 0 \text{ mM}$ ). In turn, this gradient should drive, through NHX1/2 activity, the movement of protons from the lumen to the cytosol. In agreement with this hypothesis, we detected luminal alkalization in vacuoles isolated from WT Arabidopsis in contrast to a weak acidification recorded in vacuoles from *nhx1 nhx2* mutant plants (Fig. 5). These results confirmed that NHXs are capable of moving protons into or out of the vacuole depending on the electrochemical potential of the transporter (see Notes S1 Theory).

### Phosphoinositide inhibition of NHX activity

Recently, it was hypothesized by different authors (Scholz-Starke, 2017; Pérez-Koldenkova & Hatsugai, 2017) that NHX1/2 activity might be inhibited by the phosphoinositide PI(3,5)P<sub>2</sub>, an emerging tonoplast-specific phospholipid acting as a signalling molecule in plant cells (Bak *et al.*, 2013; Carpaneto *et al.*, 2017). Our experimental approach offered a direct way to test this idea. The addition of a water-soluble form of PI(3,5)P<sub>2</sub> (Boccaccio *et al.*, 2014, see also Materials and Methods) at a concentration of 200 nM in the no K<sup>+</sup> + BTP<sup>+</sup> cytosolic solution induced a strong and reversible reduction of the acidification response mediated by NHX1/2, as shown in Fig. 6(a). We obtained a similar effect, albeit slightly milder, with PI(3,4,5)P<sub>2</sub>, but not with other two phosphoinositide species tested, PI(3,4)P<sub>2</sub> and PI(4,5)P<sub>2</sub> (Fig. 6b), suggesting that the presence of phosphate groups at the positions 3 and 5 of the inositol moiety is essential for NHX inhibition. Therefore, besides CLC-a (Carpaneto *et al.*, 2017), PI(3,5)P<sub>2</sub> also is able to affect NHX1/2 activity at similar, low nanomolar concentrations, as shown schematically in Fig. 6(c). Finally, we also tested that inositol 1,4,5 trisphosphate, InsP(3), added to the no K<sup>+</sup> + BTP<sup>+</sup> cytosolic bath solution at 2 μM concentration, had no significant effect on proton concentration changes mediated by NHX1/2 ( $\Delta[H^+]_{\text{InsP(3)}}/\Delta[H^+]_{\text{control}} = 0.98 \pm 0.01$ ,  $n = 3$ ; see also Fig. S6).

### Discussion

In this work, we extended the patch-clamp technique applied to vacuoles isolated from Arabidopsis wild-type (WT) and mutant plants by filling the patch pipette with the proton-sensitive fluorescent dye 2',7'-Bis(2-carboxyethyl)-5(6)-carboxyfluorescein (BCECF). In the whole-vacuole configuration, the proton probe diffused into the vacuolar lumen allowing to continuously monitor  $[H^+]$  variations inside the vacuole. We applied a very simple experimental protocol: starting from symmetrical concentration of potassium chloride (KCl; 100 mM) in the cytosolic bath and luminal pipette solutions, we substituted cytosolic potassium

with caesium, thereby generating a steep potassium gradient across the tonoplast. As a consequence, we could record a significant vacuolar acidification without any measurable current change (Fig. 1b). The absence of current signal was not due to a low-resolution limit in our electrophysiological system, because when we activated the vacuolar pyrophosphatase by adding inorganic pyrophosphate (PPi) in the cytosolic bath solution, proton currents could clearly be detected even with very small acidifications (Fig. 1a). Subsequent experiments using Arabidopsis *nhx1 nhx2* plants definitely demonstrated that the vacuolar acidification evoked by the potassium gradient was due to the reversible activity of NHX1/2 potassium/proton antiporters (Fig. 3a,b). Because, in physiological conditions, NHX1/2 catalyse active K<sup>+</sup> uptake into vacuoles and protons driven by these K<sup>+</sup>/H<sup>+</sup> antiporters were expected to move from the acidic vacuole to the cytosol, we verified that NHX1/2 could work in reverse mode and mediate vacuolar alkalization (Fig. 5). Our data confirmed that NHX1/2 were nonelectrogenic (Fig. 1b, middle panel) with a stoichiometry of 1 proton/ 1 potassium (or multiples), with a similar permeability for sodium and potassium ions (Fig. 2a). We also verified that they were voltage-independent (Fig. 4a) and that benzamil was a specific inhibitor (Fig. 2b). Moreover, our results illustrate the capacity of NHX antiporters to significantly impact vacuolar pH, as shown in Fig. 3, and in line with previous results with the *nhx1 nhx2* mutant (Andrés *et al.*, 2014).

Different techniques previously have been used to investigate the functional characteristics of NHX transporters. The impact of NHX activity on the formation or dissipation of proton gradients in tonoplast vesicles from plants or yeast (Barkla *et al.*, 1999; Hernández *et al.*, 2009; Barragán *et al.*, 2012) was monitored using the quenching of specific fluorophores. A similar approach was applied by using proteoliposomes (Venema *et al.*, 2002; Hernández *et al.*, 2009), which contained purified reconstituted NHX proteins. Although AtNHX1 initially was described as Na<sup>+</sup>-selective, subsequent studies have shown that tonoplast-localized NHXs are nonselective Na<sup>+</sup>,K<sup>+</sup>/H<sup>+</sup> exchangers *in vitro* (Venema *et al.*, 2002; Leidi *et al.*, 2010; Barragan *et al.*, 2012; Bassil *et al.*, 2019). However, *in vivo* they are involved primarily in vacuolar K<sup>+</sup> uptake (Leidi *et al.*, 2010; Bassil *et al.*, 2011, 2019; Barragán *et al.*, 2012; Andrés *et al.*, 2014). In Arabidopsis guard cells and roots, Na<sup>+</sup> uptake into intact vacuoles was largely independent of NHXs, suggesting that other unknown transporters were responsible for Na<sup>+</sup> entry (Andrés *et al.*, 2014; Bassil *et al.*, 2019). Heterologous expression in mutant yeast cells represented a further method to perform functional studies on NHX transporters (Quintero *et al.*, 2002; Shi *et al.*, 2002; Yokoi *et al.*, 2002); as an example, complementation of the yeast AXT3K mutant (lacking the endogenous Na<sup>+</sup> efflux proteins, ENA1-4 and NHA1, as well as the vacuolar Na<sup>+</sup>/H<sup>+</sup> antiporter NHX1) with AtNHX1 or 2 restored the ability of the yeast cells to grow in a medium enriched with NaCl or supplemented with hygromycin B (Hernández *et al.*, 2009; Barragán *et al.*, 2012). However, these approaches rely on expression in heterologous systems, or the reconstitution in highly artificial proteoliposomes and suffer from experimental constraints inherent to the assaying method. Recently, the kinetics of NHX-mediated cation uptake



has been determined using the cation-responsive fluorescent dyes PBFI (for  $K^+$ ) and SBFI (for  $Na^+$ ) loaded into intact isolated Arabidopsis vacuoles (Bassil *et al.*, 2019), but these studies also were constrained by the limited selectivity and sensitivity of these fluorochromes. In any case, it has not been possible so far to analyze the voltage-dependence of NHX transporters, the reversibility of agonist/inhibitor effects or the interplay among different proton transporters.

The technique presented here, an extension of patch-clamp, allows optimal control of the experimental conditions such as luminal/ cytosolic solutions and membrane voltage. The activity of proton-dependent tonoplast proteins can be followed in real time and their modulation by cytosolic factors can be easily investigated through changes in the external bath ionic solutions. By definition, in this technique the luminal pH is not buffered (i.e. we do not work under vacuolar pH-clamp conditions; BCECF, the only proton buffer present in the pipette solution, is 10  $\mu$ M concentration) so variations of luminal pH could activate and/or deactivate other tonoplast proteins besides the transporter under investigation. The use of specific mutant plants can help to interpret data and to correctly dissect the various contributions, which impact on the vacuolar pH. A clear example of the new possibilities offered by our approach compared to the previous techniques is given in Fig. 5, where the voltage-dependence of both NHXs and CLC-a could be investigated.

Besides plant vacuoles, the patch-clamp fluorimetry presented in this work could be extended to isolated protoplasts; however, the presence of a cell wall prevents its application in intact plant cells. The use of multi-barreled microelectrodes (see, for example, Wang *et al.*, 2015) together with genetically encoded pH- and ion-selective sensors (Bischof *et al.*, 2017; Behera *et al.*, 2018) could be the way to overcome this limitation.

In order to simulate our experimental findings, we developed a theoretical framework based on thermodynamics (see Notes S1 Theory and Figs S7–S10). We found that the kinetics of the measured signals are linked to the time required for bath perfusion and that the slower time of activation than of deactivation of the luminal proton concentration in our recordings resulted from the activity of NHXs (for detail, see Notes S1 Theory).

Interestingly, we verified that phosphoinositides (PIs) could reversibly affect NHX activity. Phosphoinositides are low-abundance phospholipids which are dynamically phosphorylated/dephosphorylated at defined positions of the inositol head group by compartment-specific lipid kinases/phosphatases. PI(3,5)P<sub>2</sub>, which is present in the membranes of yeast and plant vacuoles as well as of animal lysosomes, was a powerful inhibitor of NHX activity, as shown in Fig. 6. Further PI species were tested and simultaneous phosphorylation at positions 3 and 5 emerged as fundamental for their effectiveness. In the yeast *S. cerevisiae*, PI(3,5)P<sub>2</sub> levels increased 20-fold within minutes of hyperosmotic stress to elicit changes in the vacuolar volume (Bonangelino *et al.*, 2002). The vacuolar morphology of WT cells changed from a single large vacuole to smaller and highly fragmented vacuoles, whereas the vacuole of mutants unable to synthesize PI(3,5)P<sub>2</sub> remained unresponsive. Because the activity of yeast NHX1 is required for the fusion of vacuolar vesicles and *nhx1* mutants

have fragmented vacuoles (Qiu & Fratti, 2010), the inhibition of NHX1 by PI(3,5)P<sub>2</sub> would be coherent with the osmotic induced vacuolar fragmentation. A recent study showed that negative regulation of the yeast cation/ $H^+$  antiporter VNX1 by PI(3,5)P<sub>2</sub> contributes to the control of vacuolar  $K^+$  fluxes in yeast cells exposed to osmotic stress (Wilson *et al.*, 2018). In the light of the results presented here, it is possible that yeast VNX1 is indeed a direct target of PI(3,5)P<sub>2</sub> signalling. The Arabidopsis exchangers NHX1 and NHX2, which we show here to be targeted by PI(3,5)P<sub>2</sub>, are critically involved in the dynamic changes of volume and morphology (convolution rather than fragmentation) of guard cell vacuoles during stomatal movements (Andrés *et al.*, 2014). Mutants in the FAB1 kinases that synthesize PI(3,5)P<sub>2</sub> display aberrant vacuolar morphology (Whitley *et al.*, 2009; Hirano *et al.*, 2011), and PI(3,5)P<sub>2</sub> is required for abscisic acid (ABA)-induced vacuolar convolution and stomata closure (Bak *et al.*, 2013). Together, these data indicate an evolutionarily conserved role of PI(3,5)P<sub>2</sub> in regulating vacuolar dynamics through the regulation of ion exchangers at the tonoplast (Pérez-Koldenkova & Hatsugai, 2017). It remains to be determined whether the endosomal nonvacuolar isoforms NHX5 and NHX6, or the plasma membrane localized NHX7/SOS1 and NHX8, also are responsive to PI(3,5)P<sub>2</sub>. By contrast with vacuolar PI(3,5)P<sub>2</sub>, PI(4,5)P<sub>2</sub> is preferentially produced at the plasma membrane in response to salinity stress (van Leeuwen *et al.*, 2007), and we have shown here that PI(4,5)P<sub>2</sub> had little effect to modulate the vacuolar proteins NHX1 and NHX2. However, PI(4,5)P<sub>2</sub> is a known regulator of the mammalian plasma membrane  $Na^+/H^+$  exchanger NHE1 (reviewed by Hendus-Altenburger *et al.*, 2014), which is the animal orthologue of NHX7/SOS1. It would be interesting to test whether PI(4,5)P<sub>2</sub> specifically regulates the plasma membrane protein NHX7/SOS1. Of note is that phosphatidic acid produced by phospholipase PLD $\alpha$  in response to salt stress activates MPK6, which in turn phosphorylates and likely activates NHX7/SOS1 (Yu *et al.*, 2010), whereas ScNHX1 of *Saccharomyces cerevisiae* and EcNHX1 from the plant *Eschscholzia californica* (California golden poppy) are stimulated by lysophosphatidylcholine, another signalling lipid that is produced by plasma membrane-localized phospholipase A2 (Weigl *et al.*, 2016). These findings suggest that regulation of NHX exchangers by bioactive lipids, either directly or indirectly, is a common and physiologically relevant feature.

Because PI(3,5)P<sub>2</sub> applied at similar concentration was recently found to inhibit the activity of the proton/anion antiporter CLC-a (Carpaneto *et al.*, 2017), we can speculate that this protein could play its physiological functions together with NHXs. Their combined activity, driven by the proton motive force created by the two tonoplast proton pumps, the V-ATPase and the  $H^+$ -pyrophosphatase, has the capability to accumulate potassium-anion salts inside the vacuole. We can, then, define a Salt Accumulation Unit (SAU) formed by CLC-a with NHXs (Fig. 6c), whose capacity to increase osmolytes inside the vacuole is modulated by PI(3,5)P<sub>2</sub>. We may therefore expect that during ABA-induced stomatal closure, when PI(3,5)P<sub>2</sub> is thought to increase in guard cells (Bak *et al.*, 2013), SAU activity is inhibited to avoid futile osmolyte cycling and to allow for efficient cation and anion release from the

vacuole together with water, which would prevent a potentially damaging dehydration of the cytosol. As a consequence of the reduced activity of both CLC-a and NHXs, vacuolar pH decreases during stomatal closure (Bak *et al.*, 2013).

In summary, in this work, we show that the parallel use of electrophysiology and H<sup>+</sup> detection by fluorescence has the potential to unravel new physiological features in proton-coupled transport in plant vacuoles.


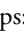


## Acknowledgements

We thank Velia Minicozzi (University of Rome, Italy) for useful discussion and Francesca Quartino (IBF-CNR, Italy) for technical assistance. This work was supported by the Italian 'Progetti di Ricerca di Interesse Nazionale' (20157955W\_003) to AC, and by grant RTI2018-094027-B-I00 from the Spanish 'Agencia Estatal de Investigación' (AEI), 'Ministerio de Ciencia, Innovación y Universidades' (MCIU), and co-financed by the European Regional Development Fund, to JMP.

## Author contributions

AG and AC designed the research; AG performed the research; AC developed the theory; AG, JSS, JMP and AC analyzed the data; and AG, JSS, JMP and AC wrote the manuscript.

## ORCID

Armando Carpaneto  <https://orcid.org/0000-0002-5060-3657>  
Antonella Gradogna  <https://orcid.org/0000-0002-4401-9913>  
José M. Pardo  <https://orcid.org/0000-0003-4510-8624>  
Joachim Scholz-Starke  <https://orcid.org/0000-0002-7376-6635>

## References

- Andrés Z, Pérez-Hormaeche J, Leidi EO, Schlücking K, Steinhorst L, McLachlan DH, Schumacher K, Hetherington AM, Kudla J, Cubero B *et al.* 2014. Control of vacuolar dynamics and regulation of stomatal aperture by tonoplast potassium uptake. *Proceedings of the National Academy of Sciences, USA* 111: E1806–E1814.
- Bak G, Lee E-J, Lee Y, Kato M, Segami S, Sze H, Maeshima M, Hwang J-U, Lee Y. 2013. Rapid structural changes and acidification of guard cell vacuoles during stomatal closure require phosphatidylinositol 3,5-bisphosphate. *The Plant Cell* 25: 2202–2216.
- Barkla BJ, Vera-Estrella R, Maldonado-Gama M, Pantoja O. 1999. Abscisic acid induction of vacuolar H<sup>+</sup>-ATPase activity in mesembryanthemum crystallinum is developmentally regulated. *Plant Physiology* 120: 811–820.
- Barragán V, Leidi EO, Andrés Z, Rubio L, De Luca A, Fernández JA, Cubero B, Pardo JM. 2012. Ion exchangers NHX1 and NHX2 mediate active potassium uptake into vacuoles to regulate cell turgor and stomatal function in Arabidopsis. *The Plant Cell* 24: 1127–1142.
- Bassil E, Tajima H, Liang Y-C, Ohto M-A, Ushijima K, Nakano R, Esumi T, Coku A, Belmonte M, Blumwald E. 2011. The Arabidopsis Na<sup>+</sup>/H<sup>+</sup> antiporters NHX1 and NHX2 control vacuolar pH and K<sup>+</sup> homeostasis to regulate growth, flower development, and reproduction. *The Plant Cell* 23: 3482–3497.
- Bassil E, Zhang S, Gong H, Tajima H, Blumwald E. 2019. Cation specificity of vacuolar NHX-type cation/H<sup>+</sup> antiporters. *Plant Physiology* 179: 616–629.
- Behera S, Zhaolong X, Luoni L, Bonza MC, Doccula FG, De Michelis MI, Morris RJ, Schwarzländer M, Costa A. 2018. Cellular Ca<sup>2+</sup> signals generate defined pH signatures in plants. *The Plant Cell* 30: 2704–2719.
- Bischof H, Rehberg M, Stryeck S, Artinger K, Eroglu E, Waldeck-Weiermair M, Gottschalk B, Rost R, Deak AT, Niedrist T *et al.* 2017. Novel genetically encoded fluorescent probes enable real-time detection of potassium in vitro and in vivo. *Nature Communications* 8: 1422.
- Boccaccio A, Scholz-Starke J, Hamamoto S, Larisch N, Festa M, Gutla PVK, Costa A, Dietrich P, Uozumi N, Carpaneto A. 2014. The phosphoinositide PI (3,5)P<sub>2</sub> mediates activation of mammalian but not plant TPC proteins: functional expression of endolysosomal channels in yeast and plant cells. *Cellular and Molecular Life Sciences* 71: 4275–4283.
- Bonangelino CJ, Nau JJ, Duex JE, Brinkman M, Wurmser AE, Gary JD, Emr SD, Weisman LS. 2002. Osmotic stress-induced increase of phosphatidylinositol 3,5-bisphosphate requires Vac14p, an activator of the lipid kinase Fab1p. *Journal of Cell Biology* 156: 1015–1028.
- Carpaneto A, Boccaccio A, Lagostena L, Di Zanni E, Scholz-Starke J. 2017. The signaling lipid phosphatidylinositol-3,5-bisphosphate targets plant CLC-a anion/H<sup>+</sup> exchange activity. *EMBO Reports* 18: 1100–1107.
- Carpaneto A, Geiger D, Bamberg E, Sauer N, Fromm J, Hedrich R. 2005. Phloem-localized, proton-coupled sucrose carrier ZmSUT1 mediates sucrose efflux under the control of the sucrose gradient and the proton motive force. *Journal of Biological Chemistry* 280: 21437–21443.
- Chanroj S, Wang G, Venema K, Zhang MW, Delwiche CF, Sze H. 2012. Conserved and diversified gene families of monovalent cation/H<sup>+</sup> antiporters from algae to flowering plants. *Frontiers in Plant Science* 3: 25.
- Costa A, Gutla PVK, Boccaccio A, Scholz-Starke J, Festa M, Basso B, Zanardi I, Pusch M, Schiavo FL, Gambale F. 2012. The Arabidopsis central vacuole as an expression system for intracellular transporters: functional characterization of the Cl<sup>-</sup>/H<sup>+</sup> exchanger CLC-7. *Journal of Physiology* 590: 3421–3430.
- De Angeli A, Monachello D, Ephritikhine G, Frachisse JM, Thomine S, Gambale F, Barbier-Brygoo H. 2006. The nitrate/proton antiporter AtCLCa mediates nitrate accumulation in plant vacuoles. *Nature* 442: 939–942.
- Festa M, Lagostena L, Carpaneto A. 2016. Using the plant vacuole as a biological system to investigate the functional properties of exogenous channels and transporters. *Biochimica et Biophysica Acta* 1858: 607–612.
- Goh C-H, Dietrich P, Steinmeyer R, Schreiber U, Nam H-G, Hedrich R. 2002. Parallel recordings of photosynthetic electron transport and K<sup>+</sup>-channel activity in single guard cells. *The Plant Journal* 32: 623–630.
- Gradogna A, Scholz-Starke J, Gutla PVK, Carpaneto A. 2009. Fluorescence combined with excised patch: measuring calcium currents in plant cation channels. *The Plant Journal* 58: 175–182.
- Hamill OP, Marty A, Neher E, Sakmann B, Sigworth FJ. 1981. Improved patch-clamp techniques for high-resolution current recording from cells and cell-free membrane patches. *Pflügers Archiv: European Journal of Physiology* 391: 85–100.
- Hendus-Altnerburger R, Kragelund BB, Pedersen SF. 2014. Structural dynamics and regulation of the mammalian SLC9A family of Na<sup>+</sup>/H<sup>+</sup> exchangers. *Current Topics in Membranes* 73: 69–148.
- Hernández A, Jiang X, Cubero B, Nieto PM, Bressan RA, Hasegawa PM, Pardo JM. 2009. Mutants of the Arabidopsis thaliana cation/H<sup>+</sup> antiporter AtNHX1 conferring increased salt tolerance in yeast: the endosome/prevacuolar compartment is a target for salt toxicity. *The Journal of Biological Chemistry* 284: 14276–14285.
- Hille B. 2001. *Ion channels of excitable membranes*. Cary, NC, USA: Oxford University Press.
- Hirano T, Matsuzawa T, Takegawa K, Sato MH. 2011. Loss-of-function and gain-of-function mutations in FAB1A/B impair endomembrane homeostasis, conferring pleiotropic developmental abnormalities in Arabidopsis. *Plant Physiology* 155: 797–807.
- Lagostena L, Festa M, Pusch M, Carpaneto A. 2017. The human two-pore channel 1 is modulated by cytosolic and luminal calcium. *Scientific Reports* 7: 43900.
- van Leeuwen W, Vermeer JEM, Gadella TWJ, Munnik T. 2007. Visualization of phosphatidylinositol 4,5-bisphosphate in the plasma membrane of suspension-cultured tobacco BY-2 cells and whole Arabidopsis seedlings. *The Plant Journal* 52: 1014–1026.

- Leidi EO, Barragán V, Rubio L, El-Hamdaoui A, Ruiz MT, Cubero B, Fernández JA, Bressan RA, Hasegawa PM, Quintero FJ *et al.* 2010. The AtNHX1 exchanger mediates potassium compartmentation in vacuoles of transgenic tomato. *The Plant Journal* **61**: 495–506.
- Neher E, Sakmann B. 1976. Single-channel currents recorded from membrane of denervated frog muscle fibres. *Nature* **260**: 799–802.
- Peiter E, Maathuis FJM, Mills LN, Knight H, Pelloux J, Hetherington AM, Sanders D. 2005. The vacuolar Ca<sup>2+</sup>-activated channel TPC1 regulates germination and stomatal movement. *Nature* **434**: 404–408.
- Pérez-Koldenkova V, Hatsugai N. 2017. Vacuolar convolution: possible mechanisms and role of phosphatidylinositol 3,5-bisphosphate. *Functional Plant Biology* **44**: 751–760.
- Qiu Q-S, Fratti RA. 2010. The Na<sup>+</sup>/H<sup>+</sup> exchanger Nhx1p regulates the initiation of *Saccharomyces cerevisiae* vacuole fusion. *Journal of Cell Science* **123**: 3266–3275.
- Quintero FJ, Ohta M, Shi H, Zhu J-K, Pardo JM. 2002. Reconstitution in yeast of the Arabidopsis SOS signaling pathway for Na<sup>+</sup> homeostasis. *Proceedings of the National Academy of Sciences, USA* **99**: 9061–9066.
- Reguera M, Bassil E, Blumwald E. 2014. Intracellular NHX-type cation/H<sup>+</sup> antiporters in plants. *Molecular Plant* **7**: 261–263.
- Sakmann B, Neher E. 1995. *Single-channel recording*. New York, NY, USA: Plenum Press.
- Scholz-Starke J. 2017. How may PI(3,5)P<sub>2</sub> impact on vacuolar acidification? *Channels* **11**: 497–498.
- Shi H, Quintero FJ, Pardo JM, Zhu J-K. 2002. The putative plasma membrane Na<sup>+</sup>/H<sup>+</sup> antiporter SOS1 controls long-distance Na<sup>+</sup> transport in plants. *The Plant Cell* **14**: 465–477.
- Venema K, Quintero FJ, Pardo JM, Donaire JP. 2002. The arabidopsis Na<sup>+</sup>/H<sup>+</sup> exchanger AtNHX1 catalyzes low affinity Na<sup>+</sup> and K<sup>+</sup> transport in reconstituted liposomes. *Journal of Biological Chemistry* **277**: 2413–2418.
- Wang Y, Dindas J, Rienmüller F, Krebs M, Waadt R, Schumacher K, Wu W-H, Hedrich R, Roelfsema MRG. 2015. Cytosolic Ca<sup>2+</sup> signals enhance the vacuolar ion conductivity of bulging Arabidopsis root hair cells. *Molecular Plant* **8**: 1665–1674.
- Weigl S, Brandt W, Langhammer R, Roos W. 2016. The Vacuolar proton-cation exchanger EcNHX1 generates pH signals for the expression of secondary metabolism in *Eschscholzia californica*. *Plant Physiology* **170**: 1135–1148.
- Whitley P, Hinz S, Doughty J. 2009. Arabidopsis FAB1/PIKfyve proteins are essential for development of viable pollen. *Plant Physiology* **151**: 1812–1822.
- Wilson ZN, Scott AL, Dowell RD, Odorizzi G. 2018. PI(3,5)P<sub>2</sub> controls vacuole potassium transport to support cellular osmoregulation. *Molecular Biology of the Cell* **29**: 1718–1731.
- Yokoi S, Quintero FJ, Cubero B, Ruiz MT, Bressan RA, Hasegawa PM, Pardo JM. 2002. Differential expression and function of *Arabidopsis thaliana* NHX Na<sup>+</sup>/H<sup>+</sup> antiporters in the salt stress response. *The Plant Journal* **30**: 529–539.
- Yoo S-D, Cho Y-H, Sheen J. 2007. Arabidopsis mesophyll protoplasts: a versatile cell system for transient gene expression analysis. *Nature Protocols* **2**: 1565–1572.
- Yu L, Nie J, Cao C, Jin Y, Yan M, Wang F, Liu J, Xiao Y, Liang Y, Zhang W. 2010. Phosphatidic acid mediates salt stress response by regulation of MPK6 in *Arabidopsis thaliana*. *New Phytologist* **188**: 762–773.

## Supporting Information

Additional Supporting Information may be found online in the Supporting Information section at the end of the article.

**Fig. S1** Schematic drawing of experimental preparation and set-up.

**Fig. S2** Loading phase of the fluorophore BCECF inside the vacuolar lumen.

**Fig. S3** Currents recorded upon replacement of cytosolic K<sup>+</sup> with BTP<sup>+</sup>.

**Fig. S4** Long-term stability of BCECF fluorescence.

**Fig. S5** Calibration of BCECF fluorescence.

**Fig. S6** Inositol 1,4,5 trisphosphate, InsP(3) had no significant effect on NHX1/2 activity.

**Fig. S7** Simulating the activity of H<sup>+</sup>-PPase in isolated vacuoles and in whole-vacuole patch-clamp configuration.

**Fig. S8** Simulating the NHX activity: effect of perfusion.

**Fig. S9** Simulating the vacuolar acidification mediated by NHXs induced by a cytosol-directed potassium gradient.

**Fig. S10** Simulating the effect of voltage and inhibitors on NHX activity.

**Notes S1 Theory** Theoretical part highlighting the fundamental elements that regulate the proton concentration in the vacuolar lumen.

Please note: Wiley Blackwell are not responsible for the content or functionality of any Supporting Information supplied by the authors. Any queries (other than missing material) should be directed to the *New Phytologist* Central Office.